PHYSICAL REVIEW D **81,** 094020 (2010)

Helicity parton distributions from spin asymmetries in W-boson production at RHIC

Daniel de Florian[1] and Werner Vogelsang[2]

[1]*Departamento de Física, FCEyN, Universidad de Buenos Aires, (1428) Pabellón 1 Ciudad Universitaria, Capital Federal, Argentina*
[2]*Institute for Theoretical Physics, Universität Tübingen, Auf der Morgenstelle 14, D-72076 Tübingen, Germany*
(Received 25 March 2010; published 19 May 2010)

We present a next-to-leading-order QCD calculation of the cross section and longitudinal spin asymmetry in single-inclusive charged-lepton production, $pp \to \ell^{\pm} X$, at the Relativistic Heavy Ion Collider, where the lepton is produced in the decay of an electroweak gauge boson. Our calculation is presented in terms of a multipurpose Monte Carlo integration program that may be readily used to include experimental spin-asymmetry data in a global analysis of helicity parton densities. We perform a toy global analysis, studying the impact of anticipated Relativistic Heavy Ion Collider data on our knowledge about the polarized antiquark distributions.

DOI: 10.1103/PhysRevD.81.094020 PACS numbers: 13.88.+e, 12.38.Bx, 13.85.Ni

I. INTRODUCTION

Despite much progress over the past three decades, many open questions concerning the helicity structure of the nucleon remain. For example, we so far have only a rather sketchy picture of the individual polarizations of the light quarks and antiquarks, $\Delta u/u$, $\Delta \bar{u}/\bar{u}$, $\Delta d/d$, $\Delta \bar{d}/\bar{d}$, where the helicity parton distributions are as usual denoted by Δq, $\Delta \bar{q}$, and their spin-averaged counterparts by q, $\bar{q}$. Since nucleons have up and down quarks as their valence quarks, the light-quark and antiquark polarizations are of much interest in QCD and play key roles in many models of nucleon structure and, more generally, for our fundamental understanding of the nucleon [1].

While lepton scattering has provided fairly precise and solid information on the ''total'' up and down distributions, $\Delta u + \Delta \bar{u}$, $\Delta d + \Delta \bar{d}$, through inclusive measurements, information on the individual Δu, $\Delta \bar{u}$, Δd, $\Delta \bar{d}$ is much more sparse and still afflicted by large uncertainties [2,3]. The tool exploited here so far has been semi-inclusive deep-inelastic scattering (SIDIS), in which one detects a specific hadron in the final state and uses the fact that the flavor content of that hadron will typically be correlated with the flavor of the quark or antiquark hit by the virtual photon in the basic deep-inelastic reaction. Measurements of SIDIS spin asymmetries have vastly improved in recent years. By now, quite precise data sets are available for various differently produced hadrons [4–8]. On the other hand, extraction of polarized parton distributions from SIDIS relies on the applicability of a leading-twist factorized QCD description of the reaction, allowing among other things the use of fragmentation functions [9] for the produced hadron determined from other processes. For the kinematics accessible in SIDIS so far one may worry if, for example, subleading twist effects can really be ignored in the theoretical analysis of the data. This leads to an uncertainty that is presently hard to quantify. It does have to be said, however, that probably for the light quarks and antiquarks, which are primarily determined from pion SIDIS, this is less of a concern. Also, thanks to the recent COMPASS measurements the kinematic reach of SIDIS data has become quite large now, extending into a regime where higher-twist effects should be less relevant. In any case, as with any measurements of nucleon structure, it is of great value to have a completely independent probe that does not involve any hadronic fragmentation and is characterized by momentum scales so large that perturbative calculations are expected to be reliable and subleading twist effects unimportant.

It has long been recognized that $W^{\pm}$ boson production at the Relativistic Heavy Ion Collider (RHIC) may provide unique and clean access to the individual helicity polarizations of quarks and antiquarks in the colliding protons [10]. Thanks to maximal violation of parity in the elementary $Wq\bar{q}'$ vertex, W bosons couple to left-handed quarks and right-handed antiquarks and hence offer direct probes of their respective helicity distributions in the nucleon. Since spin asymmetries obtained from a *single* longitudinally polarized proton beam colliding with an unpolarized beam are parity violating for sufficiently inclusive processes, they have become the prime observables in the physics program with W bosons at RHIC [10–12]:

$$A_L \equiv \frac{d\sigma^{++} + d\sigma^{+-} - d\sigma^{-+} - d\sigma^{--}}{d\sigma^{++} + d\sigma^{+-} + d\sigma^{-+} + d\sigma^{--}} \equiv \frac{d\Delta\sigma}{d\sigma}. \quad (1)$$

Here the σ^{++}, etc., denote cross sections for scattering of protons with definite helicities as indicated by the superscripts. As one can see, the helicities of the second proton are summed over, leading to the single-spin process $\vec{p}p \to W^{\pm}X$. The basic idea behind measurements of the helicity distributions at RHIC is then as follows: production of W^-, for example, selects primarily a $\bar{u}$ antiquark from one proton in conjunction with a d quark from the other. Thus, for the simple lowest-order (LO) parton-model process $d\bar{u} \to W^-$ the single-spin asymmetry becomes

$$A_L^{W^-} \approx -\frac{\Delta d(x_1^0)\bar{u}(x_2^0) - \Delta\bar{u}(x_1^0)d(x_2^0)}{d(x_1^0)\bar{u}(x_2^0) + \bar{u}(x_1^0)d(x_2^0)}, \quad (2)$$

where Δd, $\Delta \bar{u}$ denote the usual helicity distributions, probed here at a scale of the order of the W mass M_W, and where

$$x_{1,2}^0 = \frac{M_W}{\sqrt{S}} e^{\pm y_W} \tag{3}$$

with the rapidity y_W of the W bosons and the hadronic center-of-mass energy $\sqrt{S}$. It follows that at large y, where $x_1^0 \sim 1$ and $x_2^0 \ll 1$, the asymmetry will be dominated by the valence distribution probed at x_1^0 and give direct access to $-\Delta d(x_1^0, M_W^2)/d(x_1^0, M_W^2)$. Likewise, for large negative y, $A_L^{W^-}$ is given by $\Delta \bar{u}(x_1^0)/\bar{u}(x_1^0)$. The situation for W^+ follows analogously.

In practice, the above reasoning needs to be augmented in various ways. Foremost, there is an experimental issue: the detectors at RHIC are not hermetic, which means that missing-momentum techniques for the charged-lepton plus neutrino ($\ell \nu_\ell$) final states cannot be used to detect the W and reconstruct its momentum. Instead, the strategy adopted by the RHIC experiments is to detect the charged decay lepton and determine its transverse momentum p_{T_l} and rapidity η_l. The relevant process therefore becomes the single-inclusive reaction $pp \to \ell^\pm X$, similar in spirit to the processes $pp \to \pi X$, $pp \to \text{jet}X$ [13–15] used at RHIC to determine gluon polarization in the nucleon. The ensuing expression for the single-spin asymmetry for $pp \to \ell^\pm X$ differs from that in Eq. (2) even at lowest order, since the lepton transverse momentum and rapidity do not completely determine the momentum fractions of the initial partons, so that an integration over momentum fractions appears in the expression. Nevertheless, studies have shown [12,16,17] that despite this fact there should still be excellent sensitivity to the distributions Δu, $\Delta \bar{u}$, Δd, $\Delta \bar{d}$ for appropriately chosen lepton kinematics. Very recently, the RHIC collaborations have presented the first preliminary data on the cross section and single-spin asymmetry for $W^\pm$ boson production at RHIC [18,19].

There are also theoretical issues that modify the simple picture given by Eq. (2), regardless of whether one uses W or lepton kinematics. Cabibbo-suppressed contributions, which involve the polarized and unpolarized strange quark distributions, and also contributions by Z bosons, are relatively straightforward to take into account. A more important issue is the higher-order QCD corrections to the LO process $q\bar{q}' \to W^\pm$. At next-to-leading order (NLO), for example, one has the partonic reactions $q\bar{q}' \to W^\pm g$ and $qg \to W^\pm q'$. Despite the fact that the W mass sets a rather large scale so that the strong coupling constant $\alpha_s(M_W)$ is not large, the corrections can be significant and certainly need to be known for a reliable theoretical extraction of spin-dependent parton distributions from data. Consequently, a lot of theoretical work has gone into the calculation of higher-order QCD corrections to the spin asymmetries in weak-boson production at RHIC. Early work in this area [20–26] focused on the case where the W boson is detected directly, which is kinematically simpler and allows one to obtain analytical results for the NLO corrections. More recently, also an all-order resummation of terms in the partonic cross section that are logarithmically enhanced near partonic threshold was presented for this case [27]. While, as we discussed above, the direct detection of the W kinematics is not possible at RHIC, the relative size of the NLO corrections is expected to be rather independent of whether one takes into account the $W \to \ell \nu_\ell$ decay or not, since this decay does not involve any strong interactions and all QCD corrections occur only in the initial partonic state.

There have also been extensive studies of higher-order QCD corrections for the experimentally more relevant case of single-inclusive lepton production, $pp \to \ell^\pm X$. In Refs. [16,17,28] the program RHICBOS was introduced. RHICBOS is a Monte Carlo integration program for lepton distributions, specifically adapted to the polarized pp collisions at RHIC. It puts particular emphasis on the effects of soft-gluon emission and their impact on the region when the produced intermediate vector boson has small transverse momentum, q_T. In the lowest-order diagrams $q\bar{q}' \to W \to \ell \nu_\ell$, one has $q_T = 0$. Gluon radiation generates a recoil transverse momentum. When q_T tends to zero, large logarithmic corrections develop in the q_T spectrum of the W's. These can be resummed to all orders in perturbation theory, following the Collins-Soper-Sterman (CSS) formalism [29], which is done in RHICBOS at next-to-leading logarithmic level. RHICBOS is widely used for phenomenological studies related to the W program at RHIC (see, for example, Ref. [12]).

Despite this earlier work, we will present in the present paper a new NLO calculation of the cross sections and spin asymmetries for $pp \to \ell^\pm X$ at RHIC. There are several reasons why this is in our view a necessary addition. First of all, it is of value to have an independent calculation of the relevant observables at RHIC. Second, the RHIC data for the spin asymmetry in W production will ultimately need to be included in a global NLO analysis of parton distributions that includes all available information from lepton scattering and pp collisions at RHIC. Only then can the best possible information on the Δq and $\Delta \bar{q}$ be extracted. Inclusion of pp scattering data in a global analysis is a relatively complex task [2] since the computation of the parton subprocess cross-sections is typically numerically quite involved. Recent papers [2,3] used a technique based on Mellin moments [30] to achieve the first global analysis of polarized lepton scattering data and data for $pp \to \pi X$ and $pp \to \text{jet}X$ from RHIC. Our calculation presented in this paper is set up in such a way that inclusion of RHIC data for $pp \to \ell^\pm X$ will be straightforward. This is an advantage over RHICBOS, which requires prior computations of certain "grid" files for a given set of parton distribution functions, and hence is to our knowledge not readily suited for use in a global analysis code. Using our

new code, we will present in this paper a first "toy" study of a global analysis that includes projected or estimated data for W observables at RHIC.

Finally, we also have a more theory-related reason for performing a new NLO computation of the W observables at RHIC. As described above, RHICBOS includes the all-order resummation of large logarithmic corrections arising at small W transverse momentum q_T. As is well known [31], these logarithms are very relevant if one is interested, for example, in the low-transverse momentum distribution of the W boson itself. However, for the single-inclusive lepton cross section, the situation is somewhat different. q_T resummation is really only useful when the observable is *directly* sensitive to (small) q_T. For $pp \to \ell^{\pm} X$ this is the case when the measured lepton transverse momentum, p_{T_l}, is in the vicinity of $M_W/2$. This may be understood as follows: for the LO reaction $q\bar{q}' \to W \to \ell\nu_\ell$, the lepton transverse momenta are basically limited to $p_{T_l} \leq M_W/2$, except for effects related to the finite decay width of the W. This means that lepton transverse momenta $p_{T_l} > M_W/2$ primarily arise from higher-order gluon emission. Just above $M_W/2$, the lepton transverse-momentum spectrum is then dominated by the same logarithms that are present in the W transverse-momentum distribution, which are resummed by the CSS formalism. This is the motivation behind the resummation implemented in RHICBOS. In practice, however, the RHIC experiments sample over a fairly broad range of p_{T_l}. For the theoretical calculation this implies integration of the observables over p_{T_l} over this range. The broader this range, the less dominant are the soft-gluon effects addressed by resummation, and the less useful is resummation. This becomes particularly evident for the rapidity distribution of the lepton, integrated over p_{T_l}, which is the most relevant observable in W physics at RHIC and, in the spirit of Eq. (2), the best tool to separate the various polarized parton distributions. To state our point more succinctly: for practical purposes at RHIC, the region $p_{T_l} \approx M_W/2$ is only a relatively small part of the sampled kinematics, so that the q_T logarithms are not expected to dominate the observables. Their resummation is, then, not really appropriate and does not necessarily lead to an improvement of the theoretical calculation, since at the level of p_{T_l}-integrated observables there will be other higher-order effects that are of the same size as those provided by the terms logarithmic in q_T [32–34]. In any case, from the point of view of extracting polarized parton distributions, it is advisable in our view to select observables at RHIC that are insensitive to the complications associated with multiple soft-gluon emission. It therefore seems preferable to us to use a plain NLO calculation for studies of W production at RHIC, which we aim to do in this paper.

The remainder of this paper is organized as follows: in the next section we very briefly discuss our NLO calculation, which is overall quite standard. The main part of the paper is then phenomenological and presented in the following two sections. Apart from providing NLO predictions for RHIC in Sec. III, we also present in Sec. IV a "proof-of-principle" study of a global analysis involving W spin asymmetries. We finally conclude in Sec. V.

II. NEXT-TO-LEADING-ORDER CALCULATION

In order to evaluate the NLO QCD corrections to the process we rely on the version of the subtraction method introduced and extensively discussed in Refs. [35,36], and later extended to the polarized case in Ref. [14]. We refer the reader to those references for the details. Figure 1 shows some of the Feynman diagrams contributing at LO and NLO in the case of W exchange. The calculation is implemented in the Monte Carlo–like code "CHE" (standing for "Collisions at High Energies"),[1] which provides access to the full kinematics of the final-state particles, allowing the computation of any infrared-safe observable in hadronic collisions and the implementation of realistic experimental cuts. It is worth noticing that the same code can compute the unpolarized, the single-polarized, and the double-polarized cross sections.

Besides the contribution driven by W exchange, the code also allows the computation of the background arising from Z-boson and/or photon exchange at the same accuracy in perturbative QCD. We point out that at NLO the contribution from photon exchange, $q\bar{q} \to \gamma^* g$ followed by $\gamma^* \to \ell^+\ell^-$, may generate large contributions when the high-transverse momentum photon splits almost collinearly into the lepton pair, producing high-p_{T_l} leptons with a very low invariant mass. A proper treatment of this configuration would require the addition of a fragmentation contribution based on parton-to-dilepton fragmentation functions [37]. On the other hand, it is likely that configurations with two nearly collinear leptons can be distinguished experimentally from true single high-p_{T_l} leptons. In our calculation we avoid such configurations by requiring the lepton pair to have an invariant mass $M_{l_1 l_2} > 10$ GeV.

We note that we have checked the results for the spin-averaged cross section in our code against the MCFM [38] and DYNNLO [39] codes. We have also computed the fully inclusive spin-averaged and polarized W cross sections, integrated over all lepton angles. For these cross sections, analytical results are available [23–25], with which we agree.

A virtue of our code is that it lends itself to inclusion in a global analysis of polarized parton distributions, along the lines presented in Refs. [2,3]. In these papers, a method based on Mellin moments was used [30], for which the theoretical expression for any cross section is split up into parts that are independent of the parton distributions,

[1]The code is available upon request from deflo@df.uba.ar.

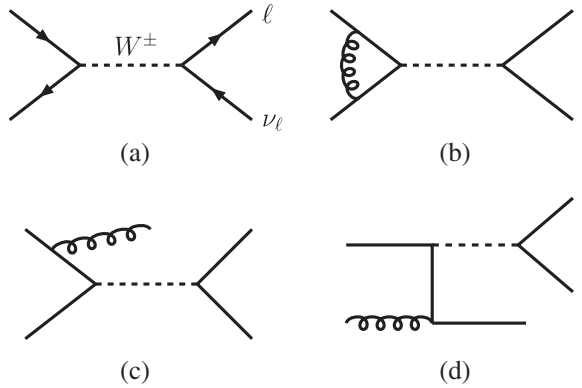

FIG. 1. Feynman diagrams for W production with leptonic decay: (a) leading order, (b) NLO virtual correction, (c) NLO real emission, (d) NLO quark-gluon scattering. Crossed diagrams are not shown.

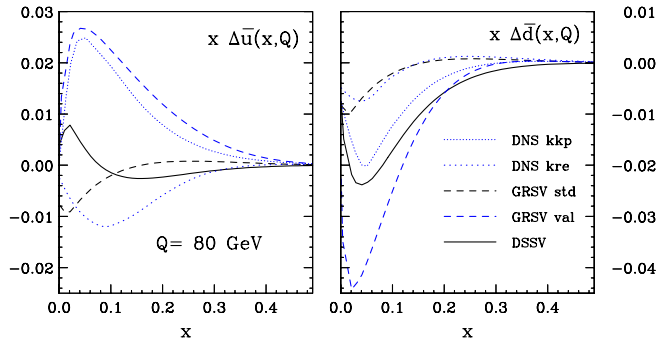

FIG. 2 (color online). Left: Next-to-leading order $x\Delta\bar{u}(x, Q)$ evaluated at the scale $Q = 80$ GeV for the DSSV [2,3] (solid lines), GRSV [40] (dashed lines), DNS-Kretzer [41] (dotted lines), and DNS-KKP (short-dashed lines) sets of polarized pdfs. Right: Same for $x\Delta\bar{d}(x, Q)$ (right-hand side).

coupled to the Mellin moments of the parton distributions. This procedure was shown to tremendously speed up the NLO fit, since the pieces that do not depend on the parton distributions, which contain the most time-consuming computations, can be calculated ''once and for all'' prior to the fit and stored as large arrays. In the actual fit one then only needs to perform numerical inverse Mellin transforms, which is straightforward. As was shown in Ref. [2], the computation of the precalculated factors is possible in a timely manner even for a code based on Monte Carlo integration, provided a proper importance sampling is used. We have implemented the corresponding strategies described in [2] in our code.

III. PHENOMENOLOGICAL RESULTS FOR RHIC

We now use our NLO code to present some numerical results for polarized pp collisions at RHIC at center-of-mass energy $\sqrt{S} = 500$ GeV. Our default choice for the spin-dependent parton distribution functions is the de Florian-Sassot-Stratmann-Vogelsang (DSSV) set [2,3]. Since we want to study the sensitivity of different observables to the polarized parton distributions, we will also consider a few other (and less recent) sets of polarized densities that primarily differ in the antiquark polarizations: the ''standard'' and ''valence'' sets from Gluck-Reya-Stratmann-Vogelsang (GRSV) [40], which have SU(2) symmetric and broken sea distributions, respectively, and the ''de_Florian-Navarro-Sassot (DNS)–Kretzer'' and ''DNS–Kniehl-Kramer-Potter (KKP)'' sets [41]. The last two sets correspond to fits to the same data for inclusive and semi-inclusive lepton scattering, but obtained using different sets of fragmentation functions [42,43] to analyze the semi-inclusive asymmetries. We note that not all of these additional sets of polarized parton distributions are completely compatible with all information now available from SIDIS. However, given the potential uncertainties in SIDIS mentioned in the Introduction, they are useful in order to gauge the sensitivity of future RHIC measurements. Figure 2 shows a comparison of the light antiquark distributions $x\Delta\bar{u}(x, Q)$ and $x\Delta\bar{d}(x, Q)$ for the various sets, evaluated at the scale $Q = 80$ GeV relevant for W production. As one can see, there are large differences among the distributions, both in qualitative behavior regarding breaking of flavor-SU(2) symmetry and in magnitude. Since all sets provide very similar results for the sum of quark and antiquark polarized distributions, $\Delta q_i + \Delta\bar{q}_i$, and since the observables are rather insensitive to the polarized gluon density, differences in the W spin asymmetries computed with the different sets can be mostly attributed to the differences in the sea distributions.

In order to compute the unpolarized cross section in the denominator of the spin asymmetries, we use the MRST2002 [44] NLO set. This choice is motivated by the fact that the MRST2002 set was also used as the ''baseline'' unpolarized set for the DSSV [2,3] spin-dependent parton distributions. We have verified that the use of more recent sets of distribution functions, like CTEQ6 [45], results in very similar cross sections.

We set the masses of the vector bosons to $M_Z = 91.1876$ GeV and $M_W = 80.398$ GeV, and the corresponding decay widths to $\Gamma_Z = 2.4952$ GeV and $\Gamma_W = 2.141$ GeV [46]. We neglect contributions from b and t quark initial states to W production and, consistent with that, use the following values for the Cabibbo-Kobayashi-Maskawa matrix elements: $|V_{ud}| = |V_{cs}| = 0.975$ and $|V_{us}| = |V_{cd}| = 0.222$. We do not include any QED or electroweak corrections, but choose the coupling constants α and $\sin^2\theta_W$ in the spirit of the ''improved Born approximation'' [47,48], in order to effectively take into account the electroweak corrections. This approach results in $\sin^2\theta_W = 0.231\,19$ and $\alpha = \alpha(M_Z) = 1/128$. We also require the lepton pair to have an invariant mass $M_{l_1 l_2} > 10$ GeV, in order to avoid potentially large NLO contributions from production of a high-p_T nearly real photon that subsequently decays into a pair of almost collinear leptons, as discussed in Sec. II.

We will study two different observables for lepton production in $pp \to \ell^{\pm} X$: the transverse-momentum (p_{T_l}) distribution of the charged lepton with a rapidity cut of $|\eta_l| < 1$, and the rapidity distribution with $p_{T_l} > 20$ GeV. We count rapidity as positive in the *forward* direction of the polarized proton. There are two hard scales in the process, which are of the same order: the mass of the gauge boson and the transverse momentum of the observed lepton. We choose $\mu_F^2 = \mu_R^2 = (M_W^2 + p_{T_l}^2)/2$ as the default factorization and renormalization scales for both the W and the Z/γ contributions. We note that the scale dependence of the cross sections and, in particular, the spin asymmetries is extremely mild in case of vector boson production, so that other choices like $\mu_F = \mu_R = M_W$ give very similar results.

We start by investigating the contribution by Z and γ exchange to the cross sections. Even though the $q\bar{q}Z$ coupling is also parity violating and hence may contribute to the single-longitudinal spin asymmetry, the Z and γ contributions are to be regarded in a sense as "dilutions" of the W signal. Being almost symmetric in ℓ^+ and ℓ^-, they will somewhat decrease the clear-cut sensitivity of A_L to the polarized sea-quark distributions, and they also contribute to the spin-averaged cross section. Figure 3 compares the Z/γ contributions (dashed lines) to the ones arising from W (solid lines), for the spin-averaged cross section as functions of rapidity (left-hand side) and transverse momentum (right-hand side). As can be observed, for positrons (upper row) the contribution from Z turns out to be rather small in the central rapidity range (about ~7%) while it does significantly add for electrons (lower row), reaching more than 40% of the W^- contribution. The effect turns out to be more noticeable at larger rapidities. We note that the $|Z|^2$ contribution dominates strongly over the γZ interference and $|\gamma|^2$ ones. In the case of the transverse-momentum distribution, the relative contribution by Z's strongly depends on p_{T_l}. Since the peak of the distribution occurs around $p_{T_l} \sim M_V/2$, with M_V the vector boson mass, the difference between the W and Z masses induces dominance of the Z contribution for $p_{T_l} \gtrsim 45$ GeV.

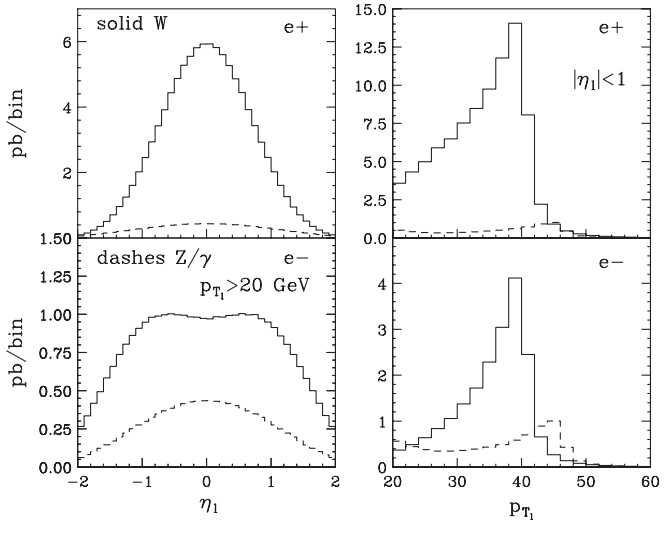

FIG. 3. Contribution from W (solid lines) and $|Z|^2 + \gamma Z + |\gamma|^2$ (dashed lines) production to the rapidity (left-hand side) and transverse-momentum (right-hand side) distributions of the leptons in spin-averaged collisions at RHIC. The upper plot corresponds to positron and the lower plot to electron production in unpolarized collisions.

The same comparison is shown in Fig. 4 for the single-polarized case, where we rely on the DSSV set of parton distributions for the polarized beam. While Z exchange can produce a single-spin cross section, its parity violation component is rather small and results in a contribution that does not exceed a few percent of the dominant W one. Of course, this does not mean that the Z contribution can be neglected in the analysis to be carried out to extract the polarized parton distributions at RHIC. The main observable is the spin asymmetry, which, at least in the case of electron production, can be considerably reduced by the Z/γ contribution in the unpolarized cross section. Vetoing events with a lepton pair could be valuable in this case in order to increase the sensitivity to the polarized parton densities. Conversely, Z bosons by themselves may offer an interesting advantage if both charged leptons from the decay $Z \to \ell^+ \ell^-$ can be detected, because in that case one can in principle reconstruct the kinematics of the Z boson, which is not possible for the W's because of the neutrino in its decay. One would then be able to directly access the momentum fractions of the parton distributions, in the spirit of Eq. (2). Unfortunately, statistics for reconstructed Z decays with both decay leptons will likely remain rather low at RHIC.

We next investigate the kinematics of W production at RHIC. In our view, it is preferable to consider distributions in lepton *rapidity*, rather than transverse momentum, since

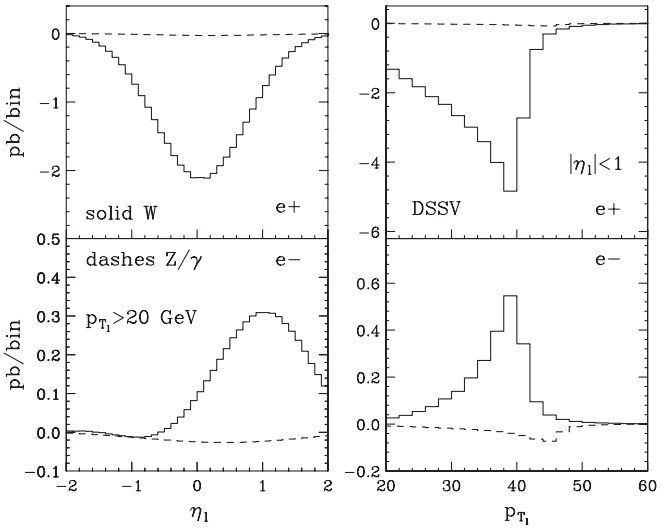

FIG. 4. Same as Fig. 3, but for single-polarized collisions using the DSSV parton distributions.

there is a particularly strong and direct correlation between lepton rapidity and the partonic momentum fractions. This correlation was already evident in the LO asymmetry as a function of the W's rapidity discussed in Eq. (2), for which we had $x_{1,2} = \frac{M_W}{\sqrt{S}} e^{\pm y_W}$. One can expect that, at least to some extent, this relation between momentum fractions and rapidity at the gauge boson level will be inherited by the lepton. Figure 5 shows the correlation between the averages of the momentum fractions, $\langle x_{1,2} \rangle$, and the rapidity of the charged lepton computed at NLO accuracy for W^- (left-hand side) and W^+ production (right-hand side) in spin-averaged collisions.[2] A remarkably strong correlation is found between $\langle x_{1,2} \rangle$ and η_l in both cases. Large *negative* lepton rapidity corresponds to *small* (*large*) momentum fractions x_1 (x_2). The opposite occurs for large positive rapidities. Actually, as a rough approximation one can parametrize these correlations by the simple "empirical" formulas

$$\langle x_{1,2} \rangle \sim \frac{M_W}{\sqrt{S}} e^{\pm \eta_l/2}. \tag{4}$$

Considering that RHIC experiments will allow one to reach rapidities of the order of $|\eta_l| \sim 2$, one can expect sensitivity to the polarized quark and antiquark distributions in the region $0.05 \lesssim x \lesssim 0.4$. We note that similar results as in Fig. 5 were also found in Ref. [17].

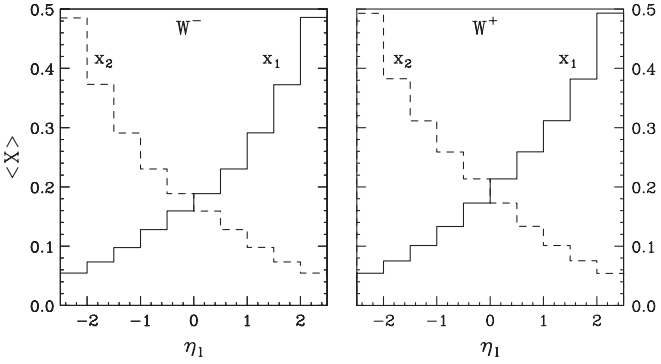

FIG. 5. Averages of the momentum fractions $x_{1,2}$ as functions of the charged lepton's rapidity η_l for W^- (left) and W^+ production (right) at RHIC.

Because of the correlation shown in Fig. 5, the combinations of parton distributions predominantly probed will vary with η_l. However, here also the underlying structure of the weak interactions enters. For W^- production, neglecting all partonic processes but the dominant $\bar{u}d \to W^- \to e^- \bar{\nu}_e$ one, the asymmetry is found to be given by

$$A_L^{e^-} \approx \frac{\int_{\otimes(x_1,x_2)} [\Delta\bar{u}(x_1) d(x_2)(1-\cos\theta)^2 - \Delta d(x_1)\bar{u}(x_2)(1+\cos\theta)^2]}{\int_{\otimes(x_1,x_2)} [\bar{u}(x_1) d(x_2)(1-\cos\theta)^2 + d(x_1)\bar{u}(x_2)(1+\cos\theta)^2]}, \tag{5}$$

where $\int_{\otimes(x_1,x_2)}$ denotes an appropriate convolution over momentum fractions, and where θ is the polar angle of the electron in the partonic center of mass system, with $\theta > 0$ in the forward direction of the polarized parton. Note that θ itself depends on the momentum fractions and on the lepton's rapidity. At large negative η_l, one has $x_2 \gg x_1$ and $\theta \sim \pi$. In this case, the first terms in the numerator and denominator of Eq. (5) strongly dominate, since the combination of parton distributions, $\Delta\bar{u}(x_1) d(x_2)$, and the angular factor, $(1-\cos\theta)^2$, each dominate over their counterpart in the second term. Therefore, the asymmetry provides a clean probe of $\Delta\bar{u}(x_1)/\bar{u}(x_1)$ at medium values of x_1. By similar reasoning, at forward rapidity $\eta_l \gg 0$ the second terms in the numerator and denominator of Eq. (5) dominate, giving access to $-\Delta d(x_1)/d(x_1)$ at relatively high x_1. For the W^+ production channel one has instead of (5)

$$A_L^{e^+} \approx \frac{\int_{\otimes(x_1,x_2)} [\Delta\bar{d}(x_1) u(x_2)(1+\cos\theta)^2 - \Delta u(x_1)\bar{d}(x_2)(1-\cos\theta)^2]}{\int_{\otimes(x_1,x_2)} [\bar{d}(x_1) u(x_2)(1+\cos\theta)^2 + u(x_1)\bar{d}(x_2)(1-\cos\theta)^2]}. \tag{6}$$

Here the distinction of the two contributions by considering large negative or positive lepton rapidities is less clear-cut than in the case of W^-. For example, at negative η_l the partonic combination $\bar{d}(x_1)u(x_2)$ will dominate, but at the same time $\theta \sim \pi$ so that the angular factor $(1+\cos\theta)^2$ given by the basic electroweak interaction is small. Likewise, at positive η_l the dominant partonic combination $\Delta u(x_1)\bar{d}(x_2)$ is suppressed by the angular factor because $\theta \sim 0$. So both terms in Eq. (6) will compete essentially for all η_l of interest. This is also the reason why the W^- cross section can become larger than the W^+ one at high rapidities (see Fig. 3). As was discussed in Refs. [49,50], the study of hadronic W decays, in particular, of charmed final states [49], might help in improving this situation.

The features displayed by Eqs. (5) and (6) are fully reflected in the behavior of the calculated NLO spin asymmetries. Figure 6 shows $A_L^{e^-}$ for electrons and $A_L^{e^+}$ for positrons at RHIC, as functions of the charged lepton's rapidity, considering only leptons arising from $W^\pm$ boson exchange. We are now using all of the sets of polarized parton distributions that we introduced earlier. The spread in the predictions for the asymmetry $A_L^{e^-}$ at $\eta_l \lesssim 0$ directly reflects the dispersion in both the absolute magnitude and sign of the different $\Delta\bar{u}(x)$ distributions shown in Fig. 2 in the range $0.05 \lesssim x \lesssim 0.2$. On the other hand, the asym-

[2]The correlation remains the same when the Z/γ contribution is included.

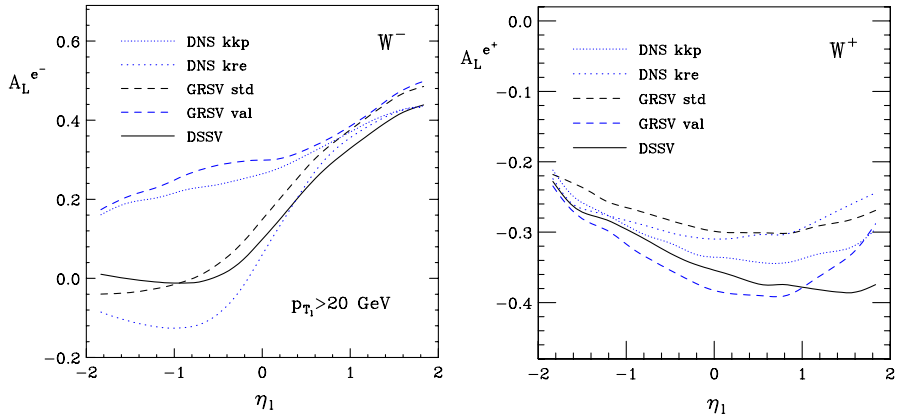

FIG. 6 (color online). Rapidity dependence of the NLO single-spin asymmetries $A_L^{e^-}$ for electrons and $A_L^{e^+}$ for positrons at RHIC, for the various sets of polarized parton distribution functions shown in Fig. 2. Only leptons produced by $W^{\pm}$ boson exchange are considered here.

metry becomes large and positive at high η_l, which reflects the fact that $\Delta d(x)$ remains negative at high x for all sets of polarized parton distributions considered here. $A_L^{e^+}$ does not show as clear features, for the reasons we just discussed. Nevertheless, at $\eta_l \gtrsim 0$ one can observe again that the spread of the predictions for the asymmetry is quite strongly correlated to the one found for the $\Delta\bar{d}$ distributions at $0.15 \lesssim x \lesssim 0.3$ in Fig. 2. Overall, the asymmetry is negative because of the contribution from Δu in Eq. (6), which is known to be positive from lepton scattering.

It is worth pointing out that in Ref. [2] spin asymmetries for the same sets of parton distributions as in Fig. 6 were shown, but at LO. Our NLO results turn out to be very close to the LO ones of [2]. This is easily understood because the bulk of the NLO corrections in the $q\bar{q}'$ channel is the same in the spin-averaged and the polarized cases, so that the corrections cancel to a high degree. This result was also observed in the study [27] of the W cross section without the leptonic decay. We do stress, however, that the individual cross sections in the numerator and the denominator of A_L receive significant NLO corrections of $\mathcal{O}(30\%)$.

For completeness, we show in Fig. 7 the asymmetries computed by including also leptons produced by Z/γ boson exchange. As expected, the inclusion of "background" leptons results in a reduction of the asymmetry due to the increase in the unpolarized cross section. Consistently with the results presented in Fig. 3, the effect is more noticeable at larger rapidities.

Figure 8 shows the spin-averaged and single-spin cross sections for electron production, as functions of p_{T_l}, integrated over $|\eta_l| \leq 1$. As expected, a peak is found around $p_{T_l} \sim M_W/2$ in both cases. For the single-polarized cross section, we are again using various sets of polarized parton distributions. One can see that the dependence on the polarized distribution functions is apparent in the magnitude of the cross section, but hardly in the shape of the transverse-momentum distribution. The latter is mainly determined by the properties of the gauge boson (like its mass and width) and general features of QCD radiation and, therefore, is very similar for both unpolarized and polarized cross sections. In other words, integration over a significant region of rapidity washes out many of the

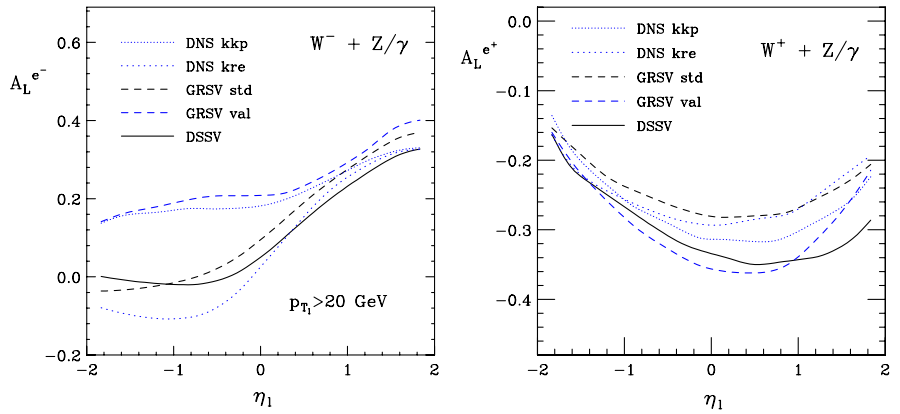

FIG. 7 (color online). Same as in Fig. 6 but including also the contribution from Z/γ exchange.

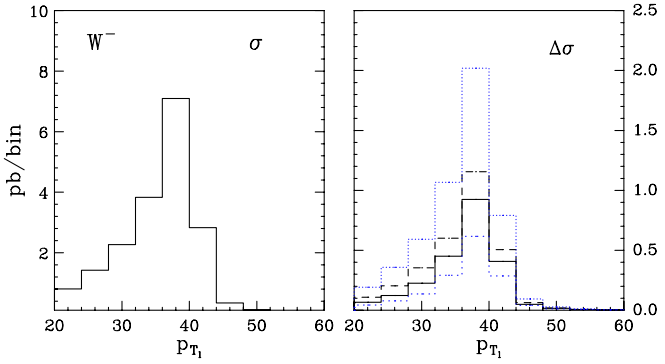

FIG. 8 (color online). Left: transverse-momentum dependence of the unpolarized cross section for electron production at RHIC. Right: same for the single-spin cross section. Here the lines follow the same pattern as in Fig. 6.

features that we found in Fig. 5 for the polarized parton distributions. While this situation may possibly be improved by integrating over noncentral regions of lepton rapidity, our studies overall confirm our expectation that in order to improve our knowledge of the polarized antiquark distributions it is preferable to study the lepton rapidity dependence of the asymmetry instead of its transverse-momentum one.

Apart from providing a good correlation between momentum fractions and lepton rapidity, another advantage of rapidity distributions integrated over a wide region of transverse momentum is that these are insensitive to soft-gluon and resummation effects. As discussed in the Introduction, the distribution near $p_{T_l} = M_W/2$ is sensitive to soft-gluon effects. Proper inclusion of these effects in the theoretical description plays a role, for example, in determinations of the W mass from the lepton p_{T_l} distributions at the Tevatron [31], or in transverse-spin studies in W boson production at RHIC [51]. The RHICBOS code [16,17] includes an all-order resummation of the next-to-leading logarithms in the W transverse momentum q_T, which are relevant near $p_{T_l} = M_W/2$. However, once one integrates over a sufficiently large region of lepton transverse momentum, these logarithms turn into finite higher-order (beyond-NLO) corrections to the transverse-momentum distribution, and neither is their resummation necessary nor is it guaranteed to provide an improved theoretical description, as there can and will be many other corrections of similar size that are not taken into account. From the point of view of extracting polarized parton distribution functions, it therefore seems advisable to us to focus on observables integrated over the lepton's transverse momentum, because these are insensitive to soft-gluon effects, and to use a plain NLO calculation. Thanks to the fact that the W mass sets a very large scale so that the strong coupling is small, and because quark antiquark annihilation is the dominant partonic channel, any "partial" beyond-NLO and nonperturbative effects remaining from q_T resummation are expected to be relatively small for such observables. Comparing the total $W^+(W^-)$ spin-averaged cross sections for $p_{T,l} > 25$ GeV and $|\eta_l| < 1$, we find 75.4 pb (17.7 pb) with our NLO code, while RHICBOS gives[3] 80.5 pb (18.8 pb). The difference will be in part due to different choices for electroweak parameters and parton distributions, but also due to the additional effects in RHICBOS just described. Somewhat larger differences between the codes occur if one considers the differential cross section at high lepton rapidity and, of course, as a function of transverse momentum at $p_{T,l} \sim M_W/2$. We have checked that these differences do not, however, significantly affect any of the previously performed sensitivity studies by the RHIC experiments.

IV. TOY ANALYSIS OF W SPIN ASYMMETRIES IN TERMS OF POLARIZED PARTON DISTRIBUTIONS

While the results presented in the previous section indicate a strong sensitivity of the single-spin asymmetries to the polarized light-quark and antiquark distributions, it is quite difficult to quantify from them the impact future RHIC measurements will have. In order to investigate this, we perform a more detailed analysis. Our strategy is to "simulate" a set of RHIC data under hopefully realistic conditions, and to add this set to the data sets included in the published DSSV [2,3] global analysis. A new fit is then performed, for which the simulated data set is included, and the impact of future W data from RHIC is gauged from the improvement found in this fit for the extracted polarized distributions. As discussed in the Introduction, knowledge about the sea-quark and antiquark polarizations in the nucleon so far comes entirely from the SIDIS spin asymmetries. In Fig. 9 we recall the DSSV results for the polarized antiquark distributions, including their respective uncertainty bands, which were obtained in DSSV by performing a Lagrangian multiplier analysis of the truncated moments $\int_{0.001}^1 dx \Delta\bar{u}(x, Q^2 = 10\,\mathrm{GeV}^2)$ and $\int_{0.001}^1 dx \Delta\bar{d}(x, Q^2 = 10\,\mathrm{GeV}^2)$, and allowing modifications of 2% in the total χ^2 of the fit.

In order to generate a simulated "RHIC data set" we proceed as follows: we compute the NLO single-longitudinal spin asymmetries $A_L^{e^+}$ and $A_L^{e^-}$ using the central DSSV set of polarized parton distributions.[4] We then randomly shift the calculated asymmetries, assuming a Gaussian distribution of their statistical uncertainties. The latter are estimated using the usual formula $\delta A_L = 1/(P\sqrt{\mathcal{L}\sigma})$. We assume a polarization of $P = 60\%$. For the integrated luminosity we consider two values: $\mathcal{L} = 200\ \mathrm{pb}^{-1}$ and $\mathcal{L} = 800\ \mathrm{pb}^{-1}$. Concerning rapidity coverage, we focus first on the present coverage for the Phenix

[3]We thank B. Surrow for providing these numbers.

[4]Asymmetries are evaluated including both W and Z/γ boson exchange contributions.

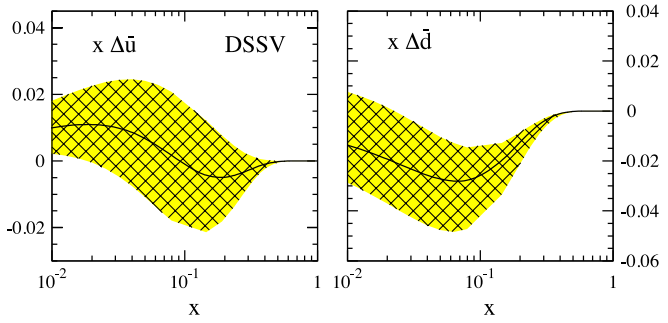

FIG. 9 (color online). $\Delta\bar{u}(x, Q^2 = 10\ \mathrm{GeV}^2)$ and $\Delta\bar{d}(x, Q^2 = 10\ \mathrm{GeV}^2)$ as obtained in the DSSV analysis [2,3]. The bands correspond to changes of 2% in the total χ^2 of the fit, as discussed in the DSSV paper.

($|\eta_l| < 0.35$) and STAR ($|\eta_l| < 1$) experiments. Later, we also investigate the impact of extended rapidity coverage as given by $|\eta_l| < 0.35$ and $1 < |\eta_l| < 2$ for Phenix[5] and $|\eta_l| < 2$ for STAR. The generated pseudodata points are shown in Fig. 10 for the two extreme scenarios (smaller luminosity and rapidity coverage vs large luminosity and rapidity coverage), along with the predictions according to the DSSV set of polarized parton distributions. We have assumed bin sizes in rapidity of $\Delta\eta_l = 0.33$, so that there are six data points in $|\eta_l| \leq 1$.

In order to perform the actual fit, we produce the precalculated grids as described in Sec. II. The choice of bins $\Delta\eta_l = 0.33$ means that we can use the same grids for both RHIC experiments, because the rapidity range covered for Phenix corresponds in good approximation to two bins with $\Delta\eta_l = 0.33$. In our first fit, we include in the DSSV analysis the pseudodata generated with the lower luminosity and the rapidity coverage presently available at RHIC. The outcome of this global fit is shown for the polarized antiquark distributions in Fig. 11, including their resulting $\Delta\chi^2/\chi^2 = 2\%$ uncertainties determined in the same way as in the published DSSV analysis. By comparing to Fig. 9, one observes that there is little modification of the actual distributions, as compared to the original DSSV ones, but a clear reduction in their uncertainty bands. This effect turns out to be very noticeable for $x \gtrsim 0.1$, as expected considering the rapidity coverage of the pseudodata added to the global fit. The decrease in the uncertainty band is also more noticeable in case of $\Delta\bar{u}$, confirming the larger sensitivity of e^- asymmetries to this distribution. At values of $x \sim 0.01$ there is almost no change in the distributions and their uncertainties, since the single-spin asymmetries at RHIC are rather insensitive to such values of x. The lower row of Fig. 12 shows the result of the corresponding fit for the larger luminosity/rapidity coverage scenario. Here the impact of RHIC data can be observed down to values of $x \sim 0.05$, thanks to the extended coverage in η_l.

[5]The upgrade planned for Phenix will actually extend the rapidity coverage to $1.2 \lesssim |\eta_l| \lesssim 2.4$.

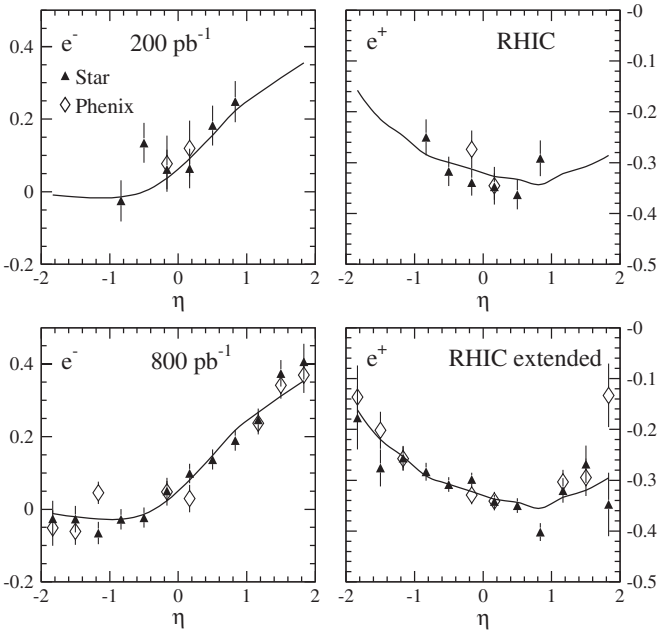

FIG. 10. Simulated data generated for e^- (left) and e^+ (right) single-spin asymmetries at STAR and Phenix for two possible extreme scenarios: integrated luminosity $\mathcal{L} = 200\ \mathrm{pb}^{-1}$ and present RHIC rapidity coverage (upper row), and integrated luminosity $\mathcal{L} = 800\ \mathrm{pb}^{-1}$ and upgraded rapidity coverage as described in the text (lower row). The "simulated data points" have been estimated by performing a NLO calculation with the DSSV set of polarized parton distributions, followed by a Gaussian shift of the points. The solid lines represent the expectation from the DSSV set.

The pseudodata used in this analysis were generated to be in full agreement, within statistical errors, with the expectation from the DSSV set. Since the latter provides an excellent description of the available SIDIS data, we have effectively assumed that constraints on the polarized parton distributions emerging from SIDIS and from W production at RHIC are in agreement. This should be the case, of course, if both are described by factorized perturbative QCD at leading power. From a theoretical point of

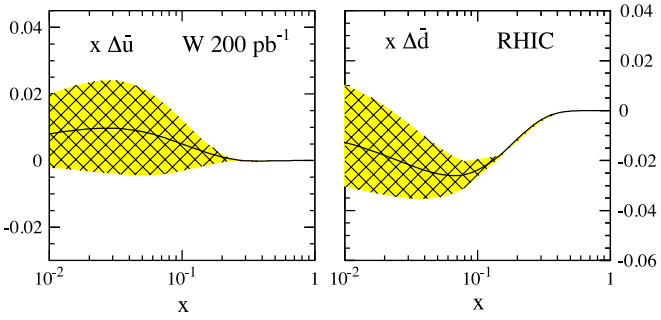

FIG. 11 (color online). Result of a global fit performed by including the simulated data generated with the lower luminosity and smaller rapidity coverage scenario (upper row in Fig. 10).

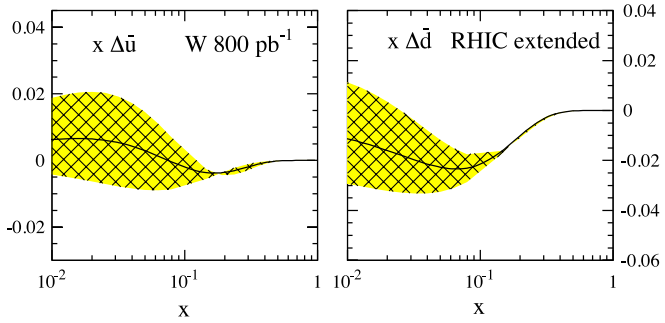

FIG. 12 (color online). Result of a global fit performed by including the simulated data generated with the larger luminosity and rapidity coverage scenario (lower row in Fig. 10).

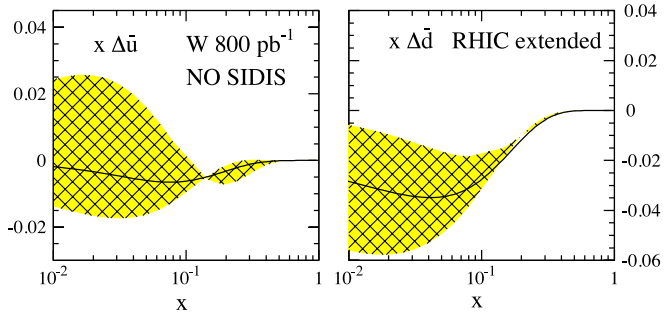

FIG. 13 (color online). Same as Fig. 12, but excluding all SIDIS data from the fit.

view, W production provides the more reliable source of information, so if any discrepancy between SIDIS and W production were found, it would likely point to higher-twist contributions in SIDIS, or ill-understood issues related to fragmentation. In this context, it is interesting to ask what the impact of future RHIC data would be if all SIDIS data were removed from the global fit. We have performed such an analysis for the scenario with larger luminosity and rapidity coverage. The result is shown in Fig. 13. We find that for $x \gtrsim 0.07$ the simulated W data put a somewhat better constraint on $\Delta\bar{u}$ and $\Delta\bar{d}$ than the SIDIS data presently do.[6] Toward smaller x, the distributions are, of course, only very loosely determined because the W spin asymmetries are not sensitive to this region. All in all, there are very good prospects for a much better determination of the polarized antiquark distributions from RHIC and SIDIS measurements.

We end by stressing that there are numerous experimental issues (like efficiencies for lepton detection, correct background subtraction, other systematic uncertainties, etc.) that have not been included in this simple analysis and that would tend to decrease the impact of the real data in the global fit. We regard this study as a "proof-of-principle" that shows that RHIC W asymmetry data can be straightforwardly included in a global analysis of polarized parton distributions. Future, more detailed, studies will need to be carried out.

V. CONCLUSIONS

We have presented a new next-to-leading-order calculation of the cross section and longitudinal spin asymmetry for the process $pp \to \ell^{\pm} X$ at RHIC, through an intermediate electroweak gauge boson. The spin asymmetry is the main probe of the light-quark and antiquark helicity distributions at RHIC. We have developed a multipurpose Monte Carlo integration program. Our code has the advantage that it allows one to directly include forthcoming RHIC data into a global analysis of spin-dependent parton densities, using the Mellin technique of [2,3,30]. Compared to the RHICBOS code [16,17], our program does not include any soft-gluon q_T-resummation effects, as we advocate the use of observables at RHIC that are insensitive to such effects. In particular, we have emphasized the advantage of the lepton rapidity distribution over the transverse-momentum one.

Our phenomenological results indicate a good sensitivity of the single-longitudinal spin asymmetries at RHIC to the light-quark and antiquark helicity distributions. This finding is in line with those of previous studies [2,12,16,17]. Contributions from Z exchange are found to be generally non-negligible. As a benchmark application of our program, we have performed a toy global analysis of "simulated" RHIC spin-asymmetry data along with the present lepton scattering and RHIC high-p_T jet and hadron data. We find that RHIC has a great potential for providing better constraints on the light-quark and antiquark helicity distributions, in particular, at moderately large momentum fractions. Once precise data becomes available from RHIC, the consistency and interplay with constraints from SIDIS will be particularly interesting to investigate. While more refined sensitivity studies will be needed, we regard our findings as a very encouraging signal that precise information on the nucleon's polarized light-quark and antiquark distributions will become available before too long. Such information will likely offer important insights into the inner structure of the nucleon and the dynamics of QCD.

ACKNOWLEDGMENTS

We are grateful to J. Haggerty, J. W. Qiu, R. Seidl, and B. Surrow for useful discussions. The work of D. d. F. has been partially supported by Conicet, UBACyT, ANPCyT, and the Guggenheim Foundation. W. V.'s work has been supported by the U.S. Department of Energy (Contract No. DE-AC02-98CH10886) and by LDRD Project No. 08-004 of Brookhaven National Laboratory.

[6]We remind the reader that the new preliminary COMPASS SIDIS data [8] were not yet included in the DSSV analysis [2,3] and are hence not included in the present study.

[1] See Sec. III.C of Ref. [2] for a discussion of the physics aspects of the light-quark and antiquark polarizations.

[2] D. de Florian, R. Sassot, M. Stratmann, and W. Vogelsang, Phys. Rev. D **80**, 034030 (2009).

[3] D. de Florian, R. Sassot, M. Stratmann, and W. Vogelsang, Phys. Rev. Lett. **101**, 072001 (2008).

[4] B. Adeva *et al.* (Spin Muon Collaboration), Phys. Lett. B **420**, 180 (1998).

[5] A. Airapetian *et al.* (HERMES Collaboration), Phys. Rev. D **71**, 012003 (2005).

[6] M. Alekseev *et al.* (COMPASS Collaboration), Phys. Lett. B **660**, 458 (2008).

[7] K. Ackerstaff *et al.* (HERMES Collaboration), Phys. Lett. B **464**, 123 (1999).

[8] O. Kouznetsov (COMPASS Collaboration), AIP Conf. Proc. **1182**, 581 (2009).

[9] D. de Florian, R. Sassot, and M. Stratmann, Phys. Rev. D **75**, 114010 (2007); **76**, 074033 (2007).

[10] C. Bourrely and J. Soffer, Phys. Lett. B **314**, 132 (1993).

[11] G. Bunce, N. Saito, J. Soffer, and W. Vogelsang, Annu. Rev. Nucl. Part. Sci. **50**, 525 (2000).

[12] G. Bunce *et al.*, "Plans for the RHIC Spin Physics Program," 2008; see spin.riken.bnl.gov/rsc.

[13] D. de Florian, Phys. Rev. D **67**, 054004 (2003); B. Jäger, A. Schäfer, M. Stratmann, and W. Vogelsang, Phys. Rev. D **67**, 054005 (2003).

[14] D. de Florian, S. Frixione, A. Signer, and W. Vogelsang, Nucl. Phys. **B539**, 455 (1999).

[15] B. Jäger, M. Stratmann, and W. Vogelsang, Phys. Rev. D **70**, 034010 (2004).

[16] P. M. Nadolsky and C. P. Yuan, Nucl. Phys. **B666**, 3 (2003).

[17] P. M. Nadolsky and C. P. Yuan, Nucl. Phys. **B666**, 31 (2003).

[18] J. Balewski and J. Stevens (STAR Collaboration), *Spring Meeting of the American Physical Society* (APS, Washington, DC, 2010).

[19] John Haggerty (Phenix Collaboration), *Spring Meeting of the American Physical Society* (APS, Washington, DC, 2010).

[20] P. Ratcliffe, Nucl. Phys. **B223**, 45 (1983).

[21] A. Weber, Nucl. Phys. **B382**, 63 (1992).

[22] A. Weber, Nucl. Phys. **B403**, 545 (1993).

[23] B. Kamal, Phys. Rev. D **53**, 1142 (1996); **57**, 6663 (1998).

[24] T. Gehrmann, Nucl. Phys. **B498**, 245 (1997).

[25] T. Gehrmann, Nucl. Phys. **B534**, 21 (1998).

[26] M. Glück, A. Hartl, and E. Reya, Eur. Phys. J. C **19**, 77 (2001).

[27] A. Mukherjee and W. Vogelsang, Phys. Rev. D **73**, 074005 (2006).

[28] See http://hep.pa.msu.edu/resum/description/rhicbos/home.html.

[29] J. C. Collins, D. E. Soper, and G. Sterman, Nucl. Phys. **B250**, 199 (1985).

[30] M. Stratmann and W. Vogelsang, Phys. Rev. D **64**, 114007 (2001).

[31] See, for example, W. Giele *et al.*, arXiv:hep-ph/0204316; T. Aaltonen *et al.* (CDF Collaboration), Phys. Rev. D **77**, 112001 (2008); V. M. Abazov *et al.* (D0 Collaboration), Phys. Rev. Lett. **103**, 141801 (2009).

[32] A. Kulesza, G. Sterman, and W. Vogelsang, Phys. Rev. D **66**, 014011 (2002).

[33] G. Bozzi, S. Catani, D. de Florian, and M. Grazzini, Nucl. Phys. **B737**, 73 (2006).

[34] G. Bozzi, S. Catani, G. Ferrera, D. de Florian, and M. Grazzini, Nucl. Phys. **B815**, 174 (2009).

[35] S. Frixione, Z. Kunszt, and A. Signer, Nucl. Phys. **B467**, 399 (1996).

[36] S. Frixione, Nucl. Phys. **B507**, 295 (1997).

[37] Z. B. Kang, J. W. Qiu, and W. Vogelsang, Phys. Rev. D **79**, 054007 (2009).

[38] See http://mcfm.fnal.gov/.

[39] S. Catani, L. Cieri, G. Ferrera, D. de Florian, and M. Grazzini, Phys. Rev. Lett. **103**, 082001 (2009).

[40] M. Glück, E. Reya, M. Stratmann, and W. Vogelsang, Phys. Rev. D **63**, 094005 (2001).

[41] D. de Florian, G. A. Navarro, and R. Sassot, Phys. Rev. D **71**, 094018 (2005).

[42] S. Kretzer, Phys. Rev. D **62**, 054001 (2000).

[43] B. A. Kniehl, G. Kramer, and B. Potter, Nucl. Phys. **B582**, 514 (2000).

[44] A. D. Martin, R. G. Roberts, W. J. Stirling, and R. S. Thorne, Eur. Phys. J. C **28**, 455 (2003).

[45] J. Pumplin, D. R. Stump, J. Huston, H. L. Lai, P. M. Nadolsky, and W. K. Tung, J. High Energy Phys. 07 (2002) 012.

[46] C. Amsler *et al.* (Particle Data Group), Phys. Lett. B **667**, 1 (2008).

[47] S. Dittmaier, M. Böhm, and A. Denner, Nucl. Phys. **B376**, 29 (1992); **B391**, 483(E) (1993).

[48] W. Beenakker *et al.*, in *Physics at LEP2*, edited by G. Altarelli, T. Sjöstrand, and F. Zwirner (CERN, Geneva, 1996).

[49] S. Arnold, A. Metz, and W. Vogelsang, *Advanced Studies Institute on Symmetries and Spin (SPIN-Praha-2007)* (European Physical Journal Special Topics, Prague, Czech Republic, 2007).

[50] E. L. Berger and P. N. Nadolsky, Phys. Rev. D **78**, 114010 (2008).

[51] Z. B. Kang and J. W. Qiu, Phys. Rev. Lett. **103**, 172001 (2009).